The AAPS Journal, Vol. 12, No. 2, June 2010 (© 2010)
DOI: 10.1208/s12248-010-9174-4

Research Article

Augmentation of Therapeutic Efficacy in Drug-Resistant Tumor Models Using Ceramide Coadministration in Temporal-Controlled Polymer-Blend Nanoparticle Delivery Systems

Lilian E. van Vlerken,[1] Zhenfeng Duan,[2] Steven R. Little,[3] Michael V. Seiden,[4] and Mansoor M. Amiji[1,5]

Received 2 September 2009; accepted 2 January 2010; published online 9 February 2010

Abstract. The development of multidrug resistance (MDR) is a major hindrance to cancer eradication as it renders tumors unresponsive to most chemotherapeutic treatments and is associated with cancer resurgence. This study describes a novel mechanism to overcome MDR through a polymer-blend nanoparticle platform that delivers a combination therapy of C6-ceramide (CER), a synthetic analog of an endogenously occurring apoptotic modulator, together with the chemotherapeutic drug paclitaxel (PTX), in a single formulation. The PTX/CER combination therapy circumvents another cellular mechanism whereby MDR develops, by lowering the threshold for apoptotic signaling. *In vivo* studies in a resistant subcutaneous SKOV3 human ovarian and in an orthotopic MCF7 human breast adenocarcinoma xenograft showed that the PTX and CER nanoparticle combination therapy reduced the final tumor volume at least twofold over treatment with the standard PTX therapy alone. The study also revealed that the cotherapy accomplished this enhanced efficacy by generating an enhancement in apoptotic signaling in both tumor types. Additionally, acute evaluation of safety with the combination therapy did not show significant changes in body weight, white blood cell counts, or liver enzyme levels. The temporal-controlled nanoparticle delivery system presented in this study allows for a simultaneous delivery of PTX + CER in breast and ovarian tumor model drug, leading to a modulation of the apoptotic threshold. This strategy has tremendous potential for effective treatment of refractory disease in cancer patients.

KEY WORDS: combination therapy; intracellular ceramide modulation; multidrug resistance; temporal-controlled polymeric nanoparticle delivery.

INTRODUCTION

In the battle against cancer, the development of multidrug resistance (MDR) poses one of the most challenging threats to treatment and is commonly implicated in tumor persistence despite invasive chemotherapy. As the term implies, MDR refers to a cross-resistance to structurally and functionally unrelated drugs, thereby rendering the tumor unresponsive to most chemotherapeutic options. In response, patients that present with the MDR phenotype are often given higher doses and/or combinations of chemotherapeutic drugs (1), still often failing to eradicate the tumor entirely. Since doses of potent cytotoxic drugs cannot be limitlessly increased, the therapeutic success at this stage hinges on strategies that will circumvent the cellular mechanisms that give rise to MDR.

Although the overexpression of the membrane-bound ATP-binding cassette drug efflux pumps (e.g., P-glycoprotein encoded by the *mdr-1* gene) is most often implicated for the occurrence of MDR, modulation of the programmed cell death (apoptosis) pathway is another likely strategy whereby tumors become chemo- and radio-resistant (2,3). Nevertheless, more than one mechanism, either simultaneous or sequential, may be responsible for the MDR phenotype observed clinically (2,3). Additionally, the low therapeutic efficacy and high systemic toxicity of combining cytotoxic drugs with P-glycoprotein modulators have led some to conclude that MDR modulation strategies are not clinically viable (4). As a result, MDR modulation strategies have shifted away from the ABC-transporter paradigm towards modulation of apoptotic signaling. Several apoptosis-modulating strategies (e.g., protein tyrosine kinase inhibitors PKI166 and ST1571, Bcl-2 antisense G-3139, and retinoids 9-cis-RA and AM-580) are currently in clinical trials, and their efficacy in MDR modulation is largely under preclinical investigation (5).

[1] Department of Pharmaceutical Sciences, School of Pharmacy, Northeastern University, 360 Huntington Avenue, Boston, Massachusetts 02115, USA.
[2] Department of Orthopedic Surgery, Massachusetts General Hospital, 55 Fruit Street, Boston, Massachusetts 02114, USA.
[3] Departments of Chemical Engineering, Bioengineering, Immunology, and The McGowan Institute of Regenerative Medicine, University of Pittsburgh, BST3 Room 5033, Pittsburgh, Pennsylvania 15260, USA.
[4] Fox Chase Cancer Center, 333 Cottman Avenue, Philadelphia, Pennsylvania 19111, USA.
[5] To whom correspondence should be addressed. (e-mail: m.amiji@neu.edu)

Over the last several years, we have suggested that a multipronged strategy that combines improvement in systemic drug delivery efficiency along with modulation of apoptotic threshold in tumors will be more beneficial in overcoming MDR than any single approach (6). We have examined the potential for exogenous C6-ceramide (CER) administration as an apoptosis-modulating strategy *in vitro* and *in vivo* (7,8), based on the principle that MDR results from decreased ceramide transport from the endoplasmic reticulum and an enhanced intracellular ceramide metabolism by the enzyme glucosylceramide synthase (GCS), thereby elevating the apoptotic threshold (9–13). Specifically, we found that a combination therapy with exogenous CER or with tamoxifen, an inhibitor of GCS, with the chemotherapeutic drug paclitaxel (PTX) was more efficacious than PTX alone (both *in vitro* and *in vivo*) in models of ovarian MDR cancer (7,8,14). Our data suggest that this therapy restores apoptotic signaling in tumor cells that are otherwise unresponsive to chemotherapy alone (7,8).

To optimize efficacy of this combination therapy, a novel polymer-blend nanoparticle was designed that includes a slow-release polymer and also a pH-responsive polymer in the same formulation, affording temporal control over release. From a unique library of polymers originally synthesized in Professor Robert Langer's lab at MIT, classified as poly(beta-amino esters) (PbAE) (15), one polymer was selected for this formulation based on its unique pH-dependant solubility properties; the polymer remains solid at pH 7.4 but rapidly dissolves at pH 6.5. Notably, this PbAE polymer efficiently associates with hydrophobic compounds during fabrication. When blended with poly (D,L-lactic co-glycolic acid) (PLGA), a heterogeneous mixture results that has a tendency to localize hydrophobic drugs (such as PTX) with the PbAE regions while more hydrophilic drugs (such as CER) localize in the PLGA matrix regions. This PLGA/PbAE blend nanoparticle was designed to immediately release PTX by rapid dissolution of PbAE in a lower-pH environment, such as the tumor microenvironment (pH < 6.5), or in the endosome/lysosome of a cell following internalization. On the other hand, CER was expected to exhibit slower release (being localized with the pH-insensitive polymer, PLGA), facilitating cellular apoptosis. To examine the therapeutic efficacy of the PTX + CER combination therapy encapsulated within 70% PLGA/30% PbAE nanoparticles, the therapy was administered *in vivo* to animals bearing orthotopic MDR human breast cancer and subcutaneous MDR human ovarian cancer. Efficacy was determined by monitoring tumor volume changes over time following a single-dose administration. Furthermore, an extensive safety evaluation was conducted *in vivo* to assess any potential toxicity of the particles upon systemic administration.

The combination PTX/CER therapeutic approach is set apart not only by the alternate approach whereby the combination therapy targets MDR but also by the distinctive polymer-blend nanoparticle that delivers the combination therapy to the tumor. In this work, a unique nanoplatform has been designed for the administration of a combination therapy with temporal control in a single formulation, a methodology that can find further use in the continuing trend with combination therapies in cancer treatment.

MATERIALS AND METHODS

Preparation and Characterization of Polymer-Blend Nanoparticle Formulations

The polymer-blend nanoparticles were manufactured by blending PLGA (mol wt. 10 kDa, 50:50 lactide-to-glycolide ratio) obtained from Birmingham Polymers (Pelham, AL, USA) with PbAE (synthesized via Michael addition reaction, Mn = 9–10 kDa) at a weight ratio of 70:30% respectively. PLGA was dissolved in acetone together with 20% (*w*/*w*) Pluronic® F-108 and 10% (*w*/*w*) CER, while PbAE was dissolved in ethanol together with 2.5% (*w*/*w*) PTX. Both preparations were heated at 37°C to facilitate dissolution, after which they were joined and instantaneously added to ten volumes water at pH 8.0 under rapid magnetic stirring. Nanoparticles were collected by centrifugation, washed with dI-H_2O at pH 8.0, and stored at 4°C. Particle size was measured by dynamic light scattering and surface charge by zeta-potential analysis. Furthermore, air-dried nanoparticle samples were visualized by scanning electron microscopy on a Hitachi S-4800 instrument, under an accelerating voltage of 3 kV. Lyophilized polymer-blend and unblended nanoparticles without Pluronic® F-108 surface modification were analyzed for surface chemistry by X-ray photoelectron spectroscopy, using a 150-eV pass energy for composition spectra and a 50-eV pass energy for high-resolution C1s scans.

Free drug treatment groups were prepared in Cremophore EL® (polyoxyethylated castor oil)/ethanol (50:50) for both PTX and CER according to the recipe for the clinical formulation of PTX. PTX was dissolved at 6 mg/ml with 527 mg of Cremophore EL® (BASF, Mount Olive, NJ, USA) and 49.7% (*v*/*v*) dehydrated alcohol USP (Thermo Fisher Scientific, Waltham, MA, USA), while CER was similarly made at 20 mg/ml.

In Vitro Drug Release Studies

In vitro drug release of 70% PLGA/30% PbAE nanoparticles was simulated by resuspending 10 mg of lyophilized nanoparticles into 5 ml phosphate-buffered saline (pH 7.4) with 0.1% Tween®-80 at pH 7.4, to simulate physiological conditions, and incubating them at 37°C. Up to 6 h, samples of release medium were collected periodically, and the volume removed was replaced with fresh medium to maintain sink conditions. At 6 h, the pH of the release medium was reduced to 6.5 to simulate the tumor environment by the addition of a predetermined amount of 1 N HCl. Following this, drug release was maintained in phosphate buffer with 0.1% Tween®-80 at pH 6.5 for the remainder of the study. Samples of release medium were again collected periodically, and release buffer was replaced. PTX release was measured by reverse-phase high-performance liquid chromatography with 50:50 acetonitrile/20 mM SDS–sodium phosphate buffer as the mobile phase. CER release was measured by incorporating 1% (*w*/*w*) NBD-CER into the nanoparticles and monitoring NBD-CER fluorescence on a plate reader at 485/530-nm excitation/emission. Drug release simulation for each nanoparticle type was performed in triplicate.

Cell Culture and Dose–Response Studies

Multidrug-resistant (*mdr-1* positive) human ovarian carcinoma cells ($SKOV3_{TR}$) and human breast carcinoma cells ($MCF7_{TR}$; kindly provided by Dr. Zhenfeng Duan at the Massachusetts General Hospital, Boston, MA, USA) were maintained in Roswell Park Memorial Institute (RPMI)-1640 (Mediatech Inc., Herndon, VA, USA) supplemented with 10% heat-inactivated fetal bovine serum (Mediatech Inc, Herndon, VA, USA) and 1% penicillin/streptomycin (Cambrex, Walkersville, MD, USA), maintained for MDR by the addition of 0.2 μM PTX (ICN, Aurora, OH, USA) in the culture medium. Wild-type (drug-sensitive) SKOV3 and MCF7 cells were similarly cultured in the absence of PTX. For dose–response studies, both drug-sensitive and MDR ovarian and breast cancer cells were harvested and plated in 96-well plates at 5,000 cells per well and treated with various doses of PTX diluted in serum-supplemented medium. Alternately, to examine the effect of a CER combination therapy alongside PTX, $SKOV3_{TR}$,and $MCF7_{TR}$ cells were similarly harvested and plated at 5,000 cells per well in 96-well plates and treated with 1 μM PTX alone or combination with 10 μM CER (Avanti Polar Lipids, Alabaster, AL, USA), whereby PTX and CER were dosed together at time zero (t_0), or the dosing of the two drugs was spaced 6 h apart. In either experiment, treatment with serum-supplemented medium was used as a negative control (0% cell death) and treatment with 50 μg/ml poly(ethylene imine) (mol. wt. 10 kDa) was used as a positive control (100% cell death). Treatment proceeded undisturbed for 6 days, after which cell viability was measured by the MTS assay (Promega, Madison, WI, USA), whereby the quantity of formazan product formed as measured, by the amount of 490-nm absorbance, is directly proportional to the remaining number of living cells. Each study was conducted with eight repetitions (well per treatment per cell type), and all studies were repeated in triplicate.

Tumor Model Development and *In Vivo* Studies

Female *nu/nu* (athymic) mice (Charles River Laboratories, Wilmington, MA, USA) were housed in sterile cages with *ad libitum* access to sterile food and acidified water on a 12:12 light/dark cycle. All experiments were approved by the Northeastern University's Animal Care and Use Committee.

$MCF7_{TR}$ tumors were inoculated, after surgical insertion of silastic estrogen implants along the right flank, by resuspending 2×10^6 cultured cells into 100 μl RPMI, with 100 μl Matrigel HC® (BD Biosciences, San Jose, CA, USA) and injecting the prep into the mammary fat pad of each anesthetized animal. Similarly, mice lacking estrogen priming were inoculated with $SKOV3_{TR}$ tumors by resuspending 4×10^6 cultured cells into 100 μl RPMI + 100 μl Matrigel HC®, injected subcutaneously into the right hind flank anesthetized animals. Once tumors had reached a palpable volume of at least 100 mm^3, mice were randomly assigned to one of five groups and subjected to a single-dose intravenous treatment of control (no treatment), PTX-free drug, PTX + CER-free drug, PTX in polymer-blend nanoparticles, and PTX + CER in polymer-blend nanoparticles, at doses of 20 mg/kg PTX and 80 mg/kg CER. Tumor volume was measured periodically with a metric caliper. Body weight was measured weekly, as was a small blood sample, collected by submandibular puncture. Whole blood was stained with crystal violet for white blood cell counts, while plasma was extracted from the remainder of the blood sample for assaying. At the end of treatment, mice were euthanized, and tumors were harvested, weighed, flash frozen, and stored at −80°C for further use.

TUNEL Staining and Protein Visualization

Tumor tissues were cryosectioned at 14-μm-thick sections and mounted onto glass slides (Superfrost Plus®, Thermo Fisher Scientific, Waltham, MA, USA). Slides were stained for the presence of fragmented DNA using a commercially available TdT-mediated dUTP nick-end labeling (TUNEL) assay (Promega, Madison, WI, USA) according to manufacturer's protocol.

P-glycoprotein and GCS expressions from $SKOV3_{TR}$ and $MCF7_{TR}$ cells were similarly visualized from basal cell extracts using the same antibodies. Protein was visualized by chemiluminescent cleavage of the horse radish peroxidase substrate. Additionally, tumor sections were also stained for the presence of either human P-glycoprotein or human GCS by immunohistochemistry, using mouse antihuman P-glycoprotein monoclonal antibody (C219) (Signet Labs, Dedham, MA, USA) or rabbit antihuman GCS polyclonal antibody (Exalpha Biochemicals, Maynard, MA, USA). The presence of antigen was then visualized with diaminobenzidine. Slides were subsequently counterstained with hematoxylin and imaged under bright-field microscopy.

Liver Enzyme Activity Measurements

As a parameter of therapeutic safety, plasma samples were assayed for the activity of alanine amino transferase (ALT) and lactate dehydrogenase (LDH). LDH activity and ALT activity were measured using commercially available kits (Quantichrom™ LDH kit, Bioassay Systems, Hayward, CA, USA and Roche Diagnostics, Basel Switzerland, respectively) according to manufacturer's protocol.

Data Analysis

Statistical analysis for all studies was performed by two-tailed, equal-variance Student t test. Statistical significance was accepted at $p<0.05$.

RESULTS

The MDR human breast ($MCF7_{TR}$) and ovarian ($SKOV3_{TR}$) cancer cell lines have been previously established by selecting cells after exposure of the wild-type cultures (MCF7 and SKOV3) to continuous and increasing concentrations of PTX. The PTX IC_{50} for the MDR ovarian subculture ($SKOV3_{TR}$) was over 100-fold higher at 1.08 μM than that of the drug-sensitive SKOV3 line, while similarly the PTX IC_{50} for the $MCF7_{TR}$ cells was tenfold higher at 0.98 μM than its drug-sensitive counterpart. To further verify that MDR phenotype was retained once the cells were xenografted *in vivo* and maintained throughout the entire study, the expression of the MDR marker proteins P-glycoprotein and

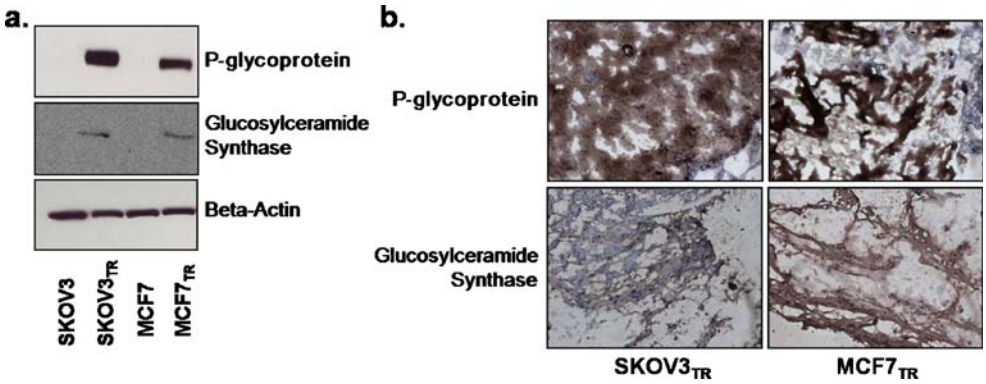

Fig. 1. Drug-resistant SKOV3 ovarian and MCF7 breast tumor models. Expression of the MDR marker proteins P-glycoprotein and glucosylceramide synthase in $SKOV3_{TR}$ and MCF_{TR} cells as compared with their wild-type cell lines **a** in culture observed by Western blot (beta-actin serves as an internal control) and **b** in xenografted tumor cross sections observed by immunohistochemistry (*brown* staining indicates the presence of P-glycoprotein or CS in the tumor tissue, while *blue* (haematoxylin) counterstaining indicate the absence of protein; ×200 original magnification)

GCS were examined. Figure 1a reveals the expression of P-glycoprotein and GCS in cultures of $SKOV3_{TR}$ and $MCF7_{TR}$ cells, alongside their wild-type, drug-sensitive, parental lines prior to xenografting them into the mice to form tumors. During the duration of tumor growth, expression of these MDR markers was retained, as seen in Fig. 1b by the evidence of P-glycoprotein and GCS staining in representative tumor tissues harvested from $SKOV3_{TR}$- and $MCF7_{TR}$-tumor-bearing mice that did not receive any treatment after a 4-week period.

Prior *in vitro* work fully examined the efficacy and mechanism of action of CER as a cotherapy to revert the MDR phenotype in these cultures (8). Cell kill efficacy of both MDR cell types increased significantly when CER was administered alongside PTX, shown in previous work to result from reduction of the apoptotic threshold in MDR cancer cells (8). It was found, however, that an interesting and important relationship existed between dosing of PTX and CER, in that cell kill efficacy increased significantly in both MDR lines when CER was administered with a delay of several hours following PTX administration; however, the converse did not hold true. For example, in $MCF7_{TR}$ cells, cell survival decreased from 60% when the drugs were coadministered to 47.1% when CER was administered 6 h following CER ($p<0.05$). Interestingly, this increase was not observed when PTX was administered with a 6-h delay following CER (61.1% cell survival) in this cell line (Table I). Similar results were seen in the $SKOV3_{TR}$ line, where dosing of CER 6 h after dosing of PTX decreased cell survival significantly (6.0% *vs.* 8.7% when the drugs were coadministered, $p<0.05$), while temporally delivering the drug in the opposite sequence did nothing to improve efficacy (Table I). Interestingly, this same temporal dosing relationship did not improve cell kill efficacy in drug-sensitive MCF7 and SKOV3 cells. In fact, sequential delivery of CER followed later by PTX reduced the efficacy of this combination therapy in the MCF7 line. While it has repeatedly been shown that a PTX + CER combination therapy also enhances chemosensitivity of drug-sensitive cells, it is hypothesized that this result is in part an additive effect of the individual toxicities of two drugs, while we have proposed a synergistic mechanism of action for the two drugs in MDR cells (14–16). This differential effect could lead to a dependence on kinetic dosing in MDR cells, while independent on kinetic dosing in the drug-sensitive population.

To incorporate this dose–kinetic relationship into the formulation, a nanoparticle system was designed that could simultaneously carry both the PTX and CER therapeutics but release each in a controlled manner within tumor cells upon uptake. In order to develop these multifunctional nanoparticles,

Table I. The Effect of Temporal Spacing Between PTX and CER on Cell Viability in MDR and Drug-Sensitive Cells

	Percent cell survival			
	SKOV3	$SKOV3_{TR}$	MCF7	$MCF7_{TR}$
PTX	35.1±1.6	50.3±8.4	43.8±2.8	87.0±7.8
CER	59.2±3.7	108±7.0	97.3±6.6	96.7±19.4
PTX + CER (t=0)	5.3±1.4	8.7±1.2	16.0±1.0	60.9±4.3
PTX (t=0) + CER (t=6)	5.7±1.0	6.0±0.8	18.9±2.3	47.1±4.3
PTX (t=6) + CER (t=0)	5.9±1.2	14.3±1.1	32.4±4.2	61.1±2.5

Percent cell survival in MDR breast and ovarian cancer cell lines, $MCF7_{TR}$ and $SKOV3_{TR}$, and their drug-sensitive parent cell lines, MCF7 and SKOV3, dosed with 1 or 0.1 μM PTX, respectively, alone or in combination with 10 μM CER, whereby the two drugs were either administered simultaneously (t=0) or sequentially with a delay of 6 h (t=6) between administration of the first drug and the second in both directions. (n=8 repeats per treatment per cell type)
PTX paclitaxel, *CER* C6-ceramide

the pH-responsive polymer PbAE was blended at 30% together with a slow-degrading polymer, PLGA, incorporated at 70%, with the intention that the polymer phases would remain immiscible, causing PbAE to form pH-responsive "pockets" or regions within the PLGA matrix (Fig. 2a), a strategy taken from previous work by Little and Langer *et al.* (16). The 70% PLGA/30% PbAE ratio was experimentally derived by blending PLGA and PbAE together in various ratios ranging from 10:90% PLGA/PbAE to 90:10% PLGA/PbAE in increments of 10%. Based on particle size and drug loading efficiency, the 70% PLGA/30% PbAE blend was chosen for development of this nanoparticle platform. In the formulation described herein, PTX was loaded into the pH-sensitive regions, while CER was loaded into the PLGA matrix, so that PTX would be rapidly released upon internalization into the tumor environment caused by the drop in pH to 6.5, and CER release would slowly follow from the PLGA matrix. Scanning electron microscopy images reveal the production of spherical particles (Fig. 2b), while dynamic light scattering measured particles at an average size of 208±6 nm. Zeta potential for these particles averaged around −26.9±5.4 mV. Chemical surface analysis revealed that, as intended, the majority of PbAE was internalized into the nanoparticle matrix, since the atomic signature of the surface of the 70% PLGA/30% PbAE nanoparticles (at 61.5±0.3% carbon, 0.8%±0.3% nitrogen, and 37.8±0.6% oxygen) resembles that of pure PLGA (58.5±0.1% carbon, 0.0±0.0% nitrogen, and 43.6±6.2% oxygen), while an even blend of the two polymers would cause a surface signature to contain even traces of both polymers. PbAE is particularly characterized by the presence of nitrogen (5.7±0.5%) in the chemical makeup, as well as a higher percentage of carbon (73.6±0.7%) and a lower percentage of oxygen (16.6±0.1%) compared with PLGA. Since few traces of this PbAE chemical signature are detected on the surface of the nanoparticles, we concluded that PbAE was internalized into the PLGA particles as designed. The drug release profile, however, was the most conclusive evidence that the nanoparticles had been developed as hypothesized (Fig. 2c). Data revealed that PTX was released more rapidly than CER and exhibited a strong pH-responsive effect, whereby the remainder of the payload was immediately released upon decrease of pH to 6.5. On the other hand, only 60% of encapsulated CER was released by the time PTX egress had expired. Moreover, CER release exhibited only a minimal pH-responsive effect, suggesting that indeed the majority of CER is associated with the PLGA matrix, whereas PTX preferentially associates with the pH-responsive PbAE matrix.

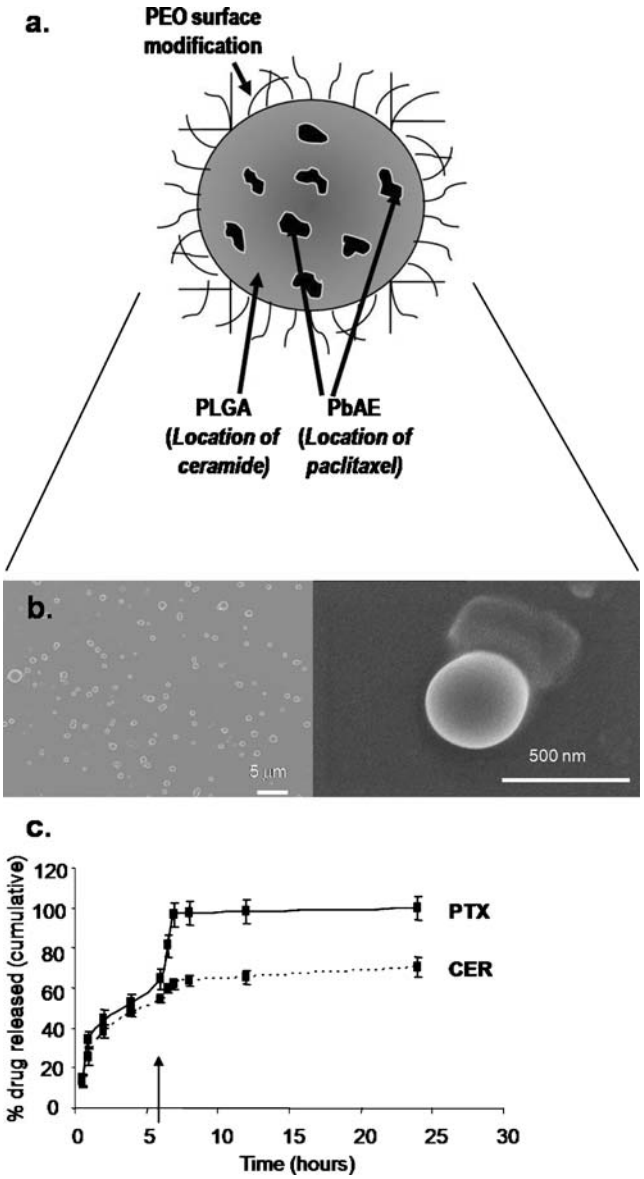

Fig. 2. PbAE/PLGA polymer-blend nanoparticles for temporal-controlled delivery. **a** Illustration of polymer-blend nanoparticle design, whereby the pH-responsive poly(beta-amino ester) (*PbAE*) internalizes into a matrix of slow-releasing poly(D,L-lactice-co-glycolide) (*PLGA*) to compartmentalize paclitaxel away from C6-ceramide within the particle, leading to controlled release of the two drugs. **b** Scanning electron micrographs of the polymer-blend nanoparticles at low resolution (*left panel*) and high resolution (*right panel*). **c** Release profile of PTX (*solid line*) and CER (*dashed line*) from the polymer-blend nanoparticles at pH 7.4 for the first 6 h and at pH 6.5 for the remainder of the release study. The *arrow* indicates a drop in pH from 7.4 to 6.5. (n=3 repeats/nanoparticle type)

SKOV3 tumor mass was established by subcutaneous administration of cells in female nude mice. On the other hand, similar to clinical forms of human breast cancer, the MCF7 cancer cell line is estrogen dependent for proliferation (17). Since intact female mice do not produce high enough estrogen levels to support MCF7 tumor development, mice must be supplied with exogenous estrogen through the insertion of continuous-release estrogen implants that maintain steady-state plasma estrogen level for at least 6 weeks. To prime the mice with sufficient estrogen to support tumor growth, silastic estradiol implants were prepared and inserted subcutaneously on the right dorsal side of intact female nu/nu mice, 48 h prior to tumor inoculation. The implants were designed to release estradiol into the bloodstream to maintain a steady-state level of 50 pg/ml for up to 6–8 weeks. While the estradiol implants indeed maintained a steady-state level at around 50 pg/ml at the start of treatment (2–3 weeks following implantation), this level had attenuated over the duration of treatment to settle at around 40 pg/ml by the end of the treatment period (data not shown).

To monitor the efficacy of this sequential PTX + CER combination treatment in blend nanoparticle formulations, tumor-bearing mice were randomly assigned to treatment with

either control (untreated), PTX (free drug) at 20 mg/kg, and PTX + CER (free drug) at 20 mg/kg and 80 mg/kg, respectively, PTX in polymer-blend nanoparticles at 20 mg/kg, and PTX + CER in polymer-blend nanoparticles. Once the tumors had reached a palpable size of at least 100 mm^3, the mice were given a single-dose intravenous injection of their assigned treatment, after which tumor volume was routinely measured with a metric Vernier caliper for 3 weeks. Figure 3 shows the therapeutic response as percent change in tumor volume over time for $SKOV3_{TR}$ tumors (Fig. 3a) and $MCF7_{TR}$ tumors (Fig. 3b). In both tumor models, the experimental PTX + CER nanoparticle therapy was most efficacious. Although the PTX + CER treatment administered as free drug showed a delay in tumor growth early on by day 4 in the $SKOV3_{TR}$ mice (Fig. 3a; 30% tumor volume change from the PTX treated groups) ,this effect was quickly lost thereafter and was entirely absent in the $MCF7_{TR}$ tumors, which were not significantly responsive to PTX + CER as free drug (Fig. 3b). Similarly, the PTX + CER nanoparticle treatment quickly regressed tumor growth by day 4 to produce a 40% lower tumor volume change compared with the PTX-treated groups. Only in this treatment group was tumor growth delay significantly retained. The therapeutic results were quite similar for the $MCF7_{TR}$ tumors (Fig. 3b). Within this treatment set, the PTX + CER nanoparticle therapy shows the greatest trend towards tumor regression with a 36% drop in tumor volume from initial, although this result is only significantly different from the remaining drug treatment groups at day 21 and not as early on as after administration as seen in the $SKOV3_{TR}$ tumors. Unlike the $SKOV3_{TR}$ tumors, the PTX + CER (free drug) treatment had no significant effect on tumor growth reduction from control or PTX alone. However, around the second week after treatment administration, the PTX + CER nanoparticle therapy did significantly decrease tumor growth when compared to the PTX + CER free drug therapy, but not when compared to the PTX alone (either as free drug or nanoparticles).

Final tumor weight, measured 28 days following treatment initiation, also revealed that the PTX + CER nanoparticle therapy was the most efficacious treatment group for both tumor types (Fig. 3c, d). At an average of 31.2±1.1 mg, the final tumor weight in the $SKOV3_{TR}$ mice after treatment with PTX/CER nanoparticles is significantly less than the final tumor weights of mice in not only the control group but also in groups that received any of the other drug treatments (PTX, PTX + CER, PTX nanoparticles; $p<0.05$, Fig. 3c). Similarly, in the $MCF7_{TR}$ breast cancer model, again the PTX + CER nanoparticle treatment resulted in the smallest final tumor weight, at 21±3 mg, which is significantly lower than the final tumor weights of the other four treatment groups (Fig. 3d). Since the mice in all the treatment groups started out with, on average, equal initial tumor volumes (~100 mm^3), it is expected that final tumor weight would correlate well to treatment efficacy. When injected intravenously in suspension, blank nanoparticles did not have any antitumor effect.

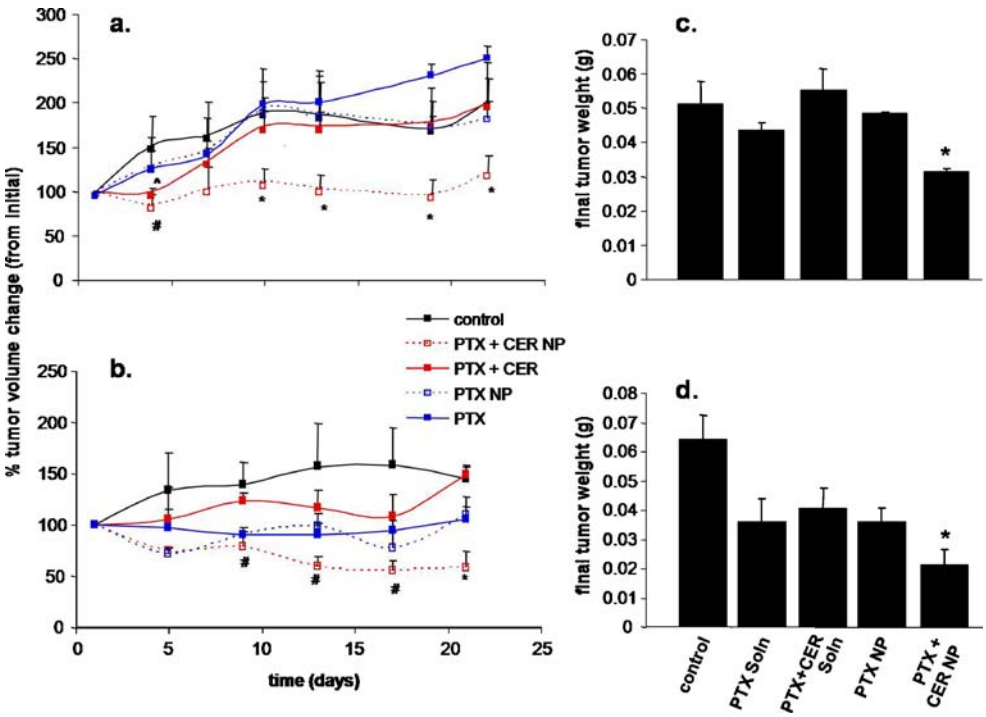

Fig. 3. Tumor growth suppression with combination PTX/CER therapy in blend nanoparticles. Tumor volume change $((V_n - V_o)/V_o \times 100\%)$ over time **a**, **b** and final tumor weights **b**, **d** following a single-dose intravenous treatment of 20 mg/kg paclitaxel (*PTX*) and/or 80 mg/kg ceramide (*CER*) administered as free drug in a Cremophore EL®-ethanol formulation or encapsulated within polymer-blend nanoparticles (*NP*) in **a**, **c** $SKOV3_{TR}$ ovarian adenocarcinoma and **b**, **d** $MCF7_{TR}$-breast-adenocarcinoma-bearing female nude mice. Control indicates no treatment. *Asterisk* indicates a significant difference ($p<0.05$) between PTX + CER NP and control, PTX, PTX NP, and PTX + CER; *Number sign* indicates a significant difference ($p<0.05$) between PTX + CER NP and control and PTX + CER. ($n=4$ mice per treatment per tumor type)

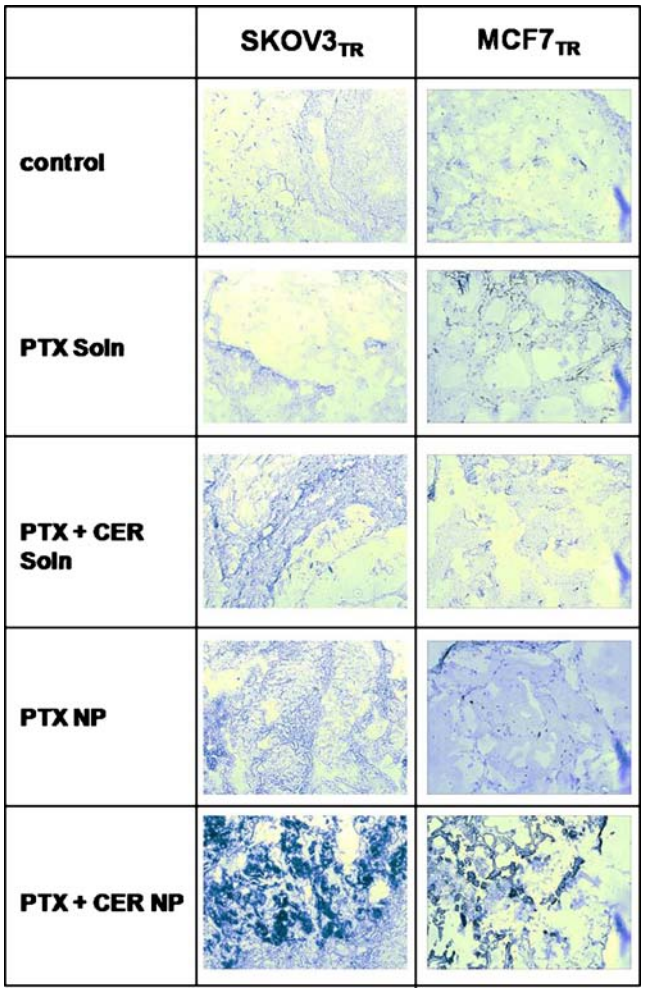

Fig. 4. Enhancement in tumor apoptotic response by TUNEL staining. Tumor TUNEL staining to indicate enhancement in apoptotic activity in $SKOV3_{TR}$ and $MCF7_{TR}$ tumor sections, harvested at day 28 following a single-dose intravenous treatment with 20 mg/kg paclitaxel (*PTX*) and/or 80 mg/kg C6-ceramide (CER) administered as free drug or within polymer-blend nanoparticles (*NP*). Control indicates no treatment. Tumors are sectioned in 12-μm sections and stained for exposed dUTP nick-end labels indicative of apoptotic activity in the tumor cells. Regions of *dark purple* staining indicate TUNEL-positive regions in the tumor section. Images are at ×200 magnification

While the tumor efficacy data on both $MCF7_{TR}$ and $SKOV3_R$ MDR models appears to support the hypothesis that the PTX + CER combination therapy delivered within the 70% PLGA/30% PbAE nanoparticles significantly enhances the ability to suppress the growth of MDR tumors, the question remains whether this therapy indeed accomplishes this feat by lowering the apoptotic threshold in MDR cancer cells, as determined in prior *in vitro* studies. To determine apoptotic activity in response to the various treatment groups, tumors harvested on day 28 after treatment were stained for apoptotic activity by TUNEL staining, which labels nick-end DNA fragments, one of the hallmarks of apoptotic activity, resulting in colorimetric output where apoptotic activity is present. Figure 4 shows stained tumor sections from $SKOV3_{TR}$ tumors and from $MCF7_{TR}$ tumors. While the free drug PTX and free drug PTX + CER treatments showed minimal TUNEL staining in their sections apart from faint indications, the PTX + CER nanoparticle therapy caused the most intense TUNEL-positive staining on all of its tumor sections in both the $SKOV3_{TR}$ and the $MCF7_{TR}$ tumors. This result appears to suggest that the combination drug therapy in the polymer-blend nanoparticles is able to restore apoptotic activity in the MDR tumor cells to overcome MDR, since apoptotic activity is most overwhelming in the PTX/CER nanoparticle-treated tumor sections, supporting the conclusion of an enhanced therapeutic efficacy associated with this treatment.

A key measure in the development of any new therapeutic is a preliminary evaluation of safety, especially with polymeric nanoparticle-based delivery. To evaluate safety and thereby any potential toxicity of the PTX + CER polymer-blend nanoparticle therapy, we examined body weight changes, white blood cell count, and serum liver enzyme activity over time following treatment initiation. Evidence for a lack of toxicity with this novel MDR therapy, changes in body weight (Table II), and white blood cell count (Table III) were also monitored for the duration of the treatment period, since significant increases in white blood cell counts and decreases in body weight are also indicative of toxicity. The lack of toxicity was verified when neither of the treatment groups causes a significant drop in body weight up to 4 weeks following treatment initiation in either $MCF7_{TR}$ and $SKOV3_{TR}$ tumor models (Table II). Even though it is observed that the Cremophore EL®-based soluble drug formulation causes a slight decrease in body weight around weeks 3 and 4 in $MCF7_{TR}$-tumor-bearing mice treated with PTX + CER or PTX administered as soluble drug, respectively, this effect can be attributed to the Cremophore EL® (a known irritant) and has no bearing on the safety of the experimental PTX/CER polymer-blend nanoparticle therapy. Table III demonstrates that there was lack of significant changes in white blood cell count following any of the treatment groups over time. No significant rises in white blood cell counts are observed in the $SKOV3_{TR}$-tumor-bearing mice following treatment with either any the experimental PTX + CER nanoparticles or any control groups. The same result was seen in the $MCF7_{TR}$ tumor model where neither treatment group exhibits a trend towards elevation of white blood cell count. However, in this $MCF7_{TR}$ model, the PTX nanoparticle treatment shows a slight elevation in white blood cell count, corresponding to the elevation of serum LDH seen in these mice (Table IV). However, this result is neither significantly elevated over basal nor significantly different from the untreated control.

A standard method to evaluate acute liver toxicity resulting from systemic administration is to monitor increases in serum enzyme activity of ALT and LDH, as these indicate any acute toxicity to the liver. Table IV shows the changes in serum ALT and LDH activity for mice bearing $SKOV3_{TR}$ and $MCF7_{TR}$ tumors. While the results suggest that there is no overall toxicity of the nanoparticles as measured by serum enzyme levels, isolated incidents exist whereby activity increases following treatment. For example, although an increase is seen in serum ALT and LDH activity at day 28 after administration of the PTX + CER soluble drug treatment in $SKOV3_{TR}$-tumor-bearing mice, this increase is not only completely absent in the $MCF7_{TR}$-tumor-bearing mice

Table II. Percent Body Weight Change Following Treatment with the Combination Therapy

Tumor type	Treatment	Body weight change (% change from initial)			
		Day 7	Day 14	Day 21	Day 28
$SKOV3_{TR}$	Control	103±1	105±2	108±2	106±2
	PTX (S)	103±2	102±2	104±2	103±3
	PTX (NP)	110±8	112±8	113±7	113±8
	PTX + CER (S)	100±3	100±3	98.5±4.4	99.8±3.0
	PTX + CER (NP)	101±1	104±2	106±1	107±2
$MCF7_{TR}$	Control	95.2±2.1	95.2±6.7	95.2±7.4	102±3
	PTX (S)	98.1±3.3	95.3±4.9	94.4±5.2	89.9±6.0
	PTX (NP)	101±0.4	102±1	102±2	93.0±9.9
	PTX + CER (S)	97.6±3.5	90.7±3.5	85.2±3.5	97.8±3.5
	PTX + CER (NP)	101±2	98.7±2.7	97.1±4.3	101±1

Average percent change in body weight over week 1 through week 4 after treatment with 20 mg/kg PTX and/or 80 mg/kg CER in solution or in polymer-blend nanoparticles as a measure of toxicity in mice bearing $SKOV3_{TR}$ ovarian adenocarcinoma and $MCF7_{TR}$ breast adenocarcinoma tumors. Control indicates no treatment. (n=4 mice per treatment per tumor type)
PTX paclitaxel, *CER* C6-ceramide, *S* solution, *NP* nanoparticles

Table III. WBC Counts Following Treatment with the Combination Therapy

Tumor type	Treatment	White blood cell count ($x10^9$ cells/L)		
		Basal	Day 14	Day 28
$SKOV3_{TR}$	Control	2.16±0.24	2.51±0.34	3.02±0.46
	PTX (S)	2.78±0.58	2.98±0.38	2.58±0.25
	PTX (NP)	3.07±0.35	2.530±0.59	3.25±0.25
	PTX + CER (S)	1.87±0.26	3.12±0.48	2.64±0.23
	PTX + CER (NP)	2.42±0.42	2.70±0.25	2.54±0.34
$MCF7_{TR}$	Control	2.83±0.28	3.81±0.974	2.83±0.52
	PTX (S)	2.22±0.58	3.32±0.89	3.17±0.96
	PTX (NP)	3.94±0.40	4.79±1.02	5.32±1.44
	PTX + CER (S)	2.85±0.43	3.20±0.31	3.01±0.41
	PTX + CER (NP)	2.72±0.76	2.97±0.35	3.17±0.77

Average WBC count at basal, day 14, and day 28 after treatment with 20 mg/kg PTX and/or 80 mg/kg CER in solution or in polymer-blend nanoparticles as a measure of toxicity in mice bearing $SKOV3_{TR}$ ovarian adenocarcinoma and $MCF7_{TR}$ breast adenocarcinoma tumors. control indicates no treatment. (n=4 mice per treatment per tumor type)
PTX paclitaxel, *CER* C6-ceramide, *S* solution, *NP* nanoparticles

Table IV. Liver Enzyme Levels Following Treatment with the Combination Therapy

Treatment group	Time point	$SKOV3_{TR}$		$MCF7_{TR}$	
		ALT (U/L)	LDH (U/L)	ALT (U/L)	LDH (U/L)
Control	Day 1	8.9±1.7	197±72	7.6±2.4	167±30
	Day 28	8.5±1.9	165±57	9.7±2.4	278±18
PTX (S)	Day 1	11.3±2.7	261±24	5.5±1.4	251±117
	Day 28	10.7±2.9	276±120	8.6±1.7	181±15
PTX (NP)	Day 1	12.8±5.7	244±63	12.1±1.8	114±32
	Day 28	9.4±1.8	364±150	6.5±0.7	122±5
PTX + CER (S)	Day 1	5.7±3.1	170±27	7.8±2.9	194±58
	Day 28	9.9±1.4	381±114	7.4±0.6	468±260
PTX + CER (NP)	Day 1	7.1±1.1	341±177	11.3±1.8	145±17
	Day 28	9.3±1.9	181±30	11.4±1.8	234±34

Serum ALT and LDH levels in $SKOV3_{TR}$- and $MCF7_{TR}$-tumor-bearing mice at day 1 of treatment and day 28 after treatment, as a measure of toxicity in response to the treatment with 20 mg/kg PTX and/or 80 mg/kg CER administered in solution or within polymer blend nanoparticles. Control indicates no treatment. (n=4 mice per treatment per tumor type)
ALT alanine aminotransferase, *LDH* lactate dehydrogenase, *PTX* paclitaxel, *CER* C6-ceramide, *S* solution, *NP* nanoparticles

but is also, in neither case, a significant change from basal level (day 1). Similarly, while the PTX nanoparticle treatment appears to double serum LDH activity by day 28 in the $MCF7_{TR}$-tumor-bearing mice, this difference is again not significant from day 1.

DISCUSSION

Although a number of therapeutic strategies have been developed to modulate the cellular mechanisms whereby MDR is thought to arise (2,18), the manipulation of the CER metabolic pathway has emerged as a promising therapeutic strategy to overcome MDR in cancer (19). Based on these findings, a therapeutic strategy that administers a combination therapy of sequentially delivered PTX and CER via novel polymeric nanoparticles was developed and characterized. Based on previous data (8), it appeared that this therapy was highly efficient to overcome MDR in *in vitro* models of breast and ovarian cancer. To test *in vivo* efficacy of this unique therapy against MDR, models of MDR human breast cancer and human ovarian cancer were developed in mice and subjected to a single-dose therapy with the experimental drug. The results demonstrate that the PTX + CER nanoparticle therapy appeared most efficacious against MDR tumors as opposed to conventional therapy. In addition to resulting in a significantly reduced tumor growth and final tumor weight in both MDR tumor models, it was also found that tumors treated with the PTX + CER nanoparticle therapy exhibited the greatest amount of apoptotic signaling, strongly suggesting that this therapy indeed overcomes MDR by restoring apoptotic signaling in tumor cells.

Upon closer examination of the tumor response to drug treatment, it appears that a single-dose administration of the PTX/CER nanoparticle therapy causes an unusually long suppression of tumor growth whereby tumor volume remains close to the original volume up until 18 days following the single-dose treatment in the $SKOV3_{TR}$ tumor model. Furthermore, tumor volume appears to decrease to 65% of its original volume in the $MCF7_{TR}$ tumor model 25 days following the single-dose treatment. Although it is unlikely that a single-dose treatment remains present in the tumor or circulation for upwards of 3 weeks, a similar single-dose treatment was as effective in retarding tumor growth over the same period of time with other studies conducted in our lab. For example, a single 20-mg/kg dose of paclitaxel in PbAE nanoparticles administered intravenously to drug-sensitive SKOV3-tumor-bearing mice suppressed tumor growth profoundly for up to 18 days, whereby tumors had increased a mere 20 mm^3 in volume (20) even though concentrations of PTX in the tumor had decreased within the first 5 h after administration (21). Even though the drugs likely only remain in the body for a minimal duration compared with the 4-week therapeutic monitoring period, the initial effect that the various treatment groups had on tumor volume can determine their subsequent rate of growth for the weeks following this single treatment.

While there are many developmental and upcoming therapeutic strategies aimed to modulate the various cellular mechanisms that give rise to MDR in cancer, this work is the first to use a novel temporal delivery strategy using a single nanoparticle drug delivery vehicle. The results presented here support the efficacy of this PTX + CER nanoparticle therapy on MDR breast and ovarian cancer, while the lack of toxicity makes it a suitable candidate for continued clinical evaluation. It is of interest to determine further whether this therapy has a similar therapeutic potential to other tumor types that present with the MDR; however, given the prevalence of MDR in breast and ovarian cancer, these results weigh heavily towards clinical potential for this therapy.

ACKNOWLEDGEMENTS

This project was supported by the National Cancer Institute's Alliance in Nanotechnology for Cancer Platform Partnership grant (R01-CA119617). Lilian E. van Vlerken was a fellow in the IGERT Nanomedical Science and Technology doctoral training program, which is jointly funded by the National Cancer Institute and the National Science Foundation. We deeply appreciate the assistance from Dr. Bo Rueda's group at the Mass General Hospital in the development of $MCF7_{TR}$ tumor model.

Competing Interests The authors declare that they have no competing interests.

Author Contributions L.E.V. carried out all the studies, analyzed the data, and wrote the first draft of the paper. Z.D. provided experimental reagents and guided the team in the analysis of results and discussions. S.R.L. provided experimental reagents and assisted with the manuscript draft. M.V.S. provided experimental reagents and guided the team in the analysis of results and discussions. M.M.A. is the principal investigator who led the research effort, provided guidance with the studies, assisted in data analysis and interpretation, and edited the manuscript.

REFERENCES

1. Bast RC, Kufe DW, Pollock RE, Weichselbaum RR, Holland JF, Frei E, *et al*. Cancer medicine. Hamilton: American Cancer Society and BC Decker; 2000.
2. Kellen JA. The reversal of multidrug resistance: an update. J Exp Ther Oncol. 2003;3:5–13.
3. Harris AL, Hochhauser D. Mechanisms of multidrug resistance in cancer treatment. Acta Oncol. 1992;31:205–13.
4. Robert J, Jarry C. Multidrug resistance reversal agents. J Med Chem. 2003;46:4805–17.
5. Tolomeo M, Simoni D. Drug resistance and apoptosis in cancer treatment: development of new apoptosis-inducing agents active in drug resistant malignancies. Curr Med Chem Anti-Canc Agents. 2002;2:387–401.
6. Jabr-Milane LS, van Vlerken LE, Yadav S, Amiji MM. Multi-functional nanocarriers to overcome tumor drug resistance. Cancer Treat Rev. 2008;34:592–602.
7. Devalapally H, Duan Z, Seiden MV, Amiji MM. Paclitaxel and ceramide co-administration in biodegradable polymeric nanoparticulate delivery system to overcome drug resistance in ovarian cancer. Int J Cancer. 2007;121:1830–8.
8. van Vlerken LE, Duan Z, Seiden MV, Amiji MM. Modulation of intracellular ceramide using polymeric nanoparticles to overcome multidrug resistance in cancer. Cancer Res. 2007;67:4843–50.
9. Liu Y-Y, Han T-Y, Giullano AE, Cabot MC. Ceramide glycosylation potentiates cellular multidrug resistance. FASEB J. 2001;15:719–30.

10. Morjani H, Aouali N, Belhoussine R, Veldman RJ, Levade T, Manfait M. Elevation of glucosylceramide in multidrug-resistant cancer cells and accumulation in cytoplasmic droplets. Int J Cancer. 2001;94:157–65.
11. Lavie Y, Cao H, Bursten SL, Giuliano AE, Cabot MC. Accumulation of glucosylceramides in multidrug-resistant cancer cells. J Biol Chem. 1996;271:19530–6.
12. Lucci A, Cho WI, Han TY, Giuliano AE, Morton DL, Cabot MC. Glucosylceramide: a marker for multiple-drug resistant cancers. Anticancer Res. 1998;18:475–80.
13. Itoh M, Kitano T, Watanabe M, Kondo T, Yabu T, Taquchi Y, *et al.* Possible role of ceramide as an indicator of chemoresistance: decrease of the ceramide content via activation of glucosylceramide synthase and sphingomyelin synthase in chemoresistant leukemia. Clin Cancer Res. 2003;9:415–23.
14. Devalapally H, Duan Z, Seiden MV, Amiji MM. Modulation of drug resistance in ovarian adenocarcinoma by enhancing intracellular ceramide using tamoxifen-loaded biodegradable polymeric nanoparticles. Clin Cancer Res. 2008;14:3193–203.
15. Lynn DM, Amiji MM, Langer R. pH-responsive polymer microspheres: rapid release of encapsulated material within the range of intracellular pH. Angew Chem Int Ed. 2001;40:1707–10.
16. Little S, Lynn DM, Ge Q, Anderson DG, Puram SV, Chen J, *et al.* Poly-beta amino ester-containing microparticles enhance the activity of nonviral genetic vaccines. Proc Natl Acad Sci. 2004;101:9534–9.
17. Leonessa F, Boulay V, Wright A, Thompson EW, Brünner N, Clarke R. The biology of breast tumor progression. Acquisition of hormone independence and resistance to cytotoxic drugs. Acta Oncol. 1992;31:115–23.
18. Szakacs G, Paterson JK, Ludwig JA, Booth-Genthe C, Gottesman MM. Targeting multidrug resistance in cancer. Nat Rev Drug Discovery. 2006;5:219–34.
19. Kolesnick R. The therapeutic potential of modulating the ceramide/sphingomyelin pathway. J Clin Invest. 2002;110:3–8.
20. Devalapally H, Shenoy D, Little S, Langer R, Amiji M. Poly (ethylene oxide)-modified poly(beta-amino ester) nanoparticles as a pH-sensitive system for tumor-targeted delivery of hydrophobic drugs: part 3 Therapeutic efficacy and safety studies in ovarian cancer xenograft model. Cancer Chemother Pharmacol. 2006;59:477–84.
21. Shenoy D, Little S, Langer R, Amiji M. Poly(ethylene oxide)-modified poly(beta amino ester) nanoparticles as a pH sensitive system for tumor-targeted delivery of hydrophobic drugs: part 2. *In vivo* distribution and tumor localization studies. Pharm Res. 2005;22:2107–14.